

CueGCL: Cluster-aware Personalized Self-Training for Unsupervised Graph Contrastive Learning

Yuecheng Li¹, Lele Fu², Sheng Huang², Chuan Chen¹, Lei Yang¹, Zibin Zheng³

¹School of Computer Science and Engineering, Sun Yat-sen University, Guangzhou 510275, China

²School of Systems Science and Engineering, Sun Yat-sen University, Guangzhou 510275, China

³School of Software Engineering, Sun Yat-Sen University, Zhuhai, 519082, China

{liyech78, fulle, huangsh253}@mail2.sysu.edu.cn, {chenchuan, yanglei39, zhzibin}@mail.sysu.edu.cn,

Abstract

Recently, graph contrastive learning (GCL) has emerged as one of the optimal solutions for node-level and supervised tasks. However, for structure-related and unsupervised tasks such as graph clustering, current GCL algorithms face difficulties acquiring the necessary cluster-level information, resulting in poor performance. In addition, general unsupervised GCL improves the performance of downstream tasks by increasing the number of negative samples, which leads to severe class collision and unfairness of graph clustering. To address the above issues, we propose a **Cluster-aware Graph Contrastive Learning Framework (CueGCL)** to jointly learn clustering results and node representations. Specifically, we design a *personalized self-training (PeST)* strategy for unsupervised scenarios, which enables our model to capture precise cluster-level personalized information. With the benefit of the PeST, we alleviate class collision and unfairness without sacrificing the overall model performance. Furthermore, *aligned graph clustering (AGC)* is employed to obtain the cluster partition, where we align the clustering space of our downstream task with that in PeST to achieve more consistent node embeddings. Finally, we theoretically demonstrate the effectiveness of our model, showing it yields an embedding space with a significantly discernible cluster structure. Extensive experimental results also show our CueGCL exhibits state-of-the-art performance on five benchmark datasets with different scales.

1 Introduction

With the development of the information age, data with complicated relationships have emerged in large quantities, such as social networks. Graph clustering (Community detection) [Li *et al.*, 2024a; Deng *et al.*, 2024] is an essential task in complex network analysis.

Recently, graph representation learning has become an important backbone for graph clustering that incorporates network topology and node attributes [Xiao *et al.*, 2024]. Especially, graph contrastive learning (GCL) is a superior

technique to enhance the discriminability of nodes in graph representation learning by comparing positive and negative samples. It has demonstrated remarkable success in semi-supervised downstream tasks such as node classification [Li *et al.*, 2022], graph classification [Li *et al.*, 2024b], and link prediction [Zhang *et al.*, 2023]. Nonetheless, within the context of graph representation learning utilizing GCL, two significant challenges persist:

Challenge I Cluster-Level Awareness of Graphs

Some structure-related and unsupervised learning tasks in network analysis also attract much attention, such as graph clustering. **Most graph contrastive learning frameworks have difficulty learning the structural information required in these problems.** They focus only on node-level similarity but fail to consider the cluster structure in the graph when sampling positive and negative node pairs. To further illustrate the importance of cluster-level information, we use t-SNE to visualize node representations from a novel GCL algorithm *gCool* [Li *et al.*, 2022] and our *CueGCL* in Figure 1, and report their accuracy (ACC) of graph clustering. *gCool* is a Graph Communal Contrastive Learning algorithm that can learn both node representations and community partition. Compared with Figures 1(b) and 1(c), we observe that the node representation space of *gCool* does not have good community properties, and also its clustering accuracy is significantly lower than ours. Specifically, our model pays attention to learning the personalized features of each community to obtain a compact embedding space within the clusters, also as shown in Figure 4, but existing methods fail to do so.

N_{neg}	50	100	500	1000	1500
Micro-F1	32.3	23.4	18.1	6.9	4.6
Macro-F1	31.3	25.5	19.3	5.4	3.9
Number of nodes in 4 th clu	380	343	54	34	5
time / epoch (s)	0.6	0.7	0.9	1.0	1.2

Table 1: Effect of negative sample size on contrastive-based models in graph clustering task on Citeseer.

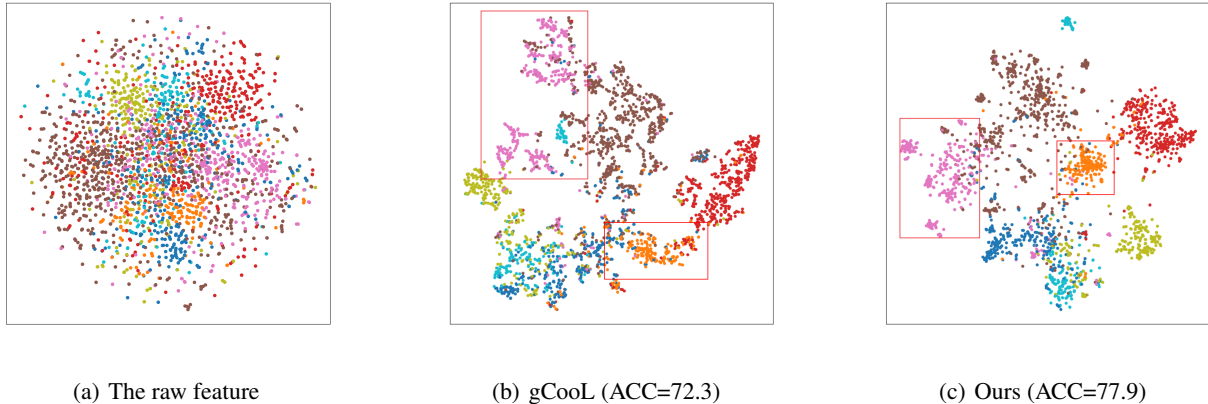


Figure 1: The t-SNE visualizations on Cora. (a) is the visualization for raw node features. (b) is the visualization for the node representations from gCooL. (c) is the visualization for the node representations from our CueGCL. The node representations generated by our CueGCL are more distinguishable than the gCooL.

Challenge II Fair Awareness for Each Cluster

Some contrastive-based methods typically require a large number of negative samples, allowing for uniform separation of representations across all samples. However, the contrast of large negative samples would inevitably lead to the class collision issue, which means that different samples from the same class are treated as negative sample pairs and pushed away incorrectly [Saunshi *et al.*, 2019]. Moreover, we find that **class collision induces unfairness in unsupervised graph clustering, which lacks label information to mitigate bias in negative sampling of GCL compared to supervised downstream tasks**. Specifically, certain clusters may not be aware of the model, leading to inaccurate detection. To further explain, we conduct graph clustering with the general GCL model on Citeseer and report the experimental results in Table 1. We empirically observe that as the negative sample size (i.e. denoted as N_{neg}) increases, the F1 score shows a substantial decrease. Furthermore, the number of nodes that the model marks as the fourth cluster (i.e. $4^{th} clu$), named 'ML', on the Citeseer keeps decreasing. This means that almost all nodes in the 'ML' cluster (actually should be 596) are pulled into other clusters by the contrastive-based model because they are incorrectly identified as negative sample pairs. A good model should fairly perceive each cluster in the graph, meaning that the accuracy of any single cluster should not be significantly lower than that of other clusters or the overall clustering accuracy of the graph. Overall, we conclude that the contrastive-based model cannot fairly perceive each cluster in the network.

To address the above challenges, we propose a novel GCL method, called **Community-aware Graph Contrastive Learning (CueGCL)**.

The main contributions of our paper are summarized as follows:

- We present an end-to-end graph contrastive learning

framework, called CueGCL, that jointly trains cluster partition and node embeddings.

- We propose a personalized self-training (PeST) strategy for unsupervised scenarios that allows our model to actively learn the personalized features of each cluster. Moreover, it is theoretically demonstrated that our PeST strategy adaptively results in a more compact internal structure of each cluster.
- We point out that our PeST module is actually more unbiased for negative sampling, thereby effectively alleviating the class collision problem. Furthermore, by incorporating balanced sampling in PeST, our model enhances its fair aware ability for each cluster.
- Experimental results over the five benchmark datasets indicate that our CueGCL outperforms the state-of-the-art. Moreover, the effectiveness of our model for mitigating the unfairness problem is verified.

2 Related Work

Graph Contrastive Learning. Graph contrastive learning is a powerful self-supervised learning technique that focuses on learning representations of nodes in the semantic space by comparing positive and negative samples. Contrasts between positive samples enable representations to learn consistency across different views of similar samples, while contrasts with negative samples emphasize the differences between different classes of samples. DGI [Velickovic *et al.*, 2019] uses an objective function based on mutual information rather than random walking, which applies the ideas of DIM [Hjelm *et al.*, 2018] to graph data so that the node representations contain global graph information. MVGRL [Hassani and Khasahmadi, 2020] introduces different structural views of a graph based on DGI for learning both node-level and graph-level representations. GRACE [Zhu *et al.*, 2020] proposes a simplified contrastive framework by using InfoNCE

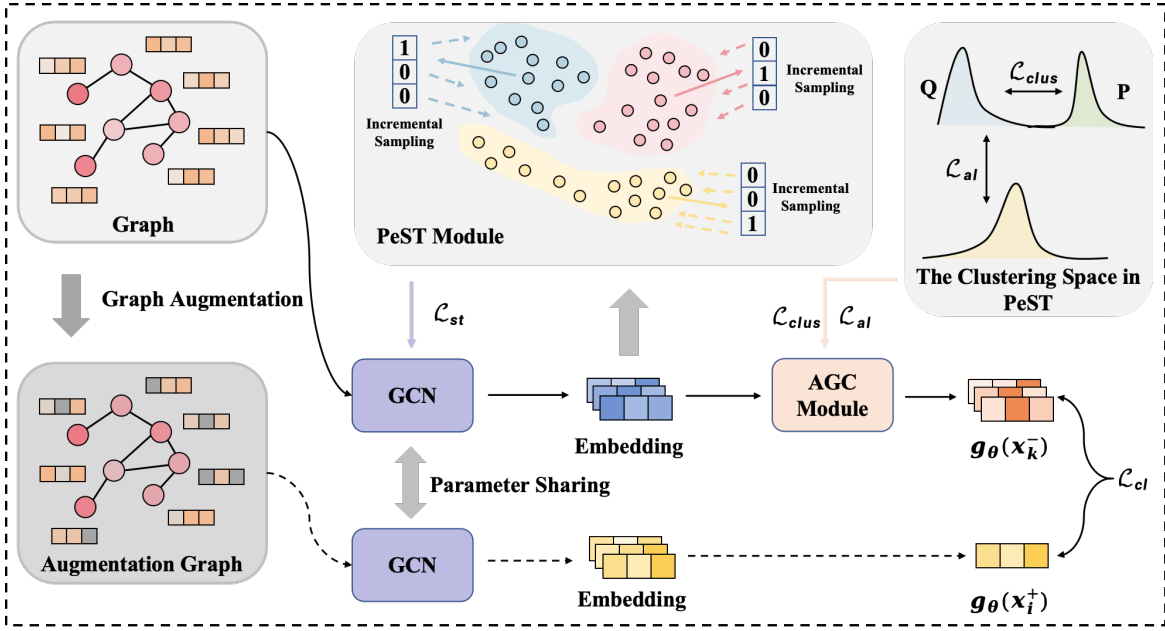


Figure 2: The overall framework of our CueGCL. It consists of three parts: graph contrastive learning framework, personalized self-training (PeST) module, and aligned graph clustering (AGC) module. In our framework, we use the feature-space graph augmentation strategy, where x_i^+ represents the positive sample and x_k^- represents the negative sample if $k \in \tilde{N}_i$. The clustering results and node embeddings are both optimized by objective functions: \mathcal{L}_{cl} , \mathcal{L}_{st} , \mathcal{L}_{clus} and \mathcal{L}_{al} .

loss [Oord *et al.*, 2018] with both inter-view and intra-view negative pairs. BGRL [Thakoor *et al.*, 2021] introduces a graph self-supervised learning method that uses two encoders to generate node representations without negative samples. However, most non-contrastive methods still depend on complex architectures or dataset-specific augmentations [Shiao *et al.*, 2023]. Overall, above mentioned contrastive-based methods are not suitable for graph clustering directly as they only focus on node-level or graph-level representation learning and ignore the specific cluster structure of the network.

Deep Graph Clustering. More recently, graph representation learning combined with clustering algorithms has become a popular trend in graph clustering. MinCutPool [Bianchi *et al.*, 2020] proposes a continuous relaxation graph pooling method that leverages GNNs to learn node clustering, avoiding the computational cost of spectral decomposition. DMoN [Tsitsulin *et al.*, 2023] presents a novel GNN pooling method that optimizes modularity for efficient unsupervised graph clustering. ARVGA [Pan *et al.*, 2018] uses a graph autoencoder to map the node on the attribute graph into a compact representation, and combines an adversarial training module to make it conform to a prior distribution. VGAER [Qiu *et al.*, 2022] proposes a variational graph autoencoder for reconstruction-based graph clustering, and gives its non-probabilistic version. However, such reconstruction-based algorithms extract features at a fine granularity, so they are unsuitable for downstream node-level tasks, e.g., node classification and clustering. CommDGI [Zhang *et al.*, 2020] introduces the trainable clustering layer and community-oriented objectives, which learns the community-related node representations through joint optimization. GDCL [Zhao *et al.*,

2021] combines a clustering layer with the contrastive learning framework, which utilizes a debiased negative sampling strategy to reduce the false negative samples. gCool [Li *et al.*, 2022] proposes the reweighted self-supervised cross-contrastive training module to reduce the bias in contrastive learning using community information. S^3 -CL [Ding *et al.*, 2023] infers node clusters and prototypes, and enforces nodes in the same cluster to group around their corresponding prototypes in the latent space. However, graph prototypical contrastive learning does not account for the sampling bias in positives. Moreover, strictly enforcing intra-cluster compactness may reduce the continuity and generalization capability of the representation space. In general, the existing graph representation algorithms based on contrastive learning do not solve the class collision and unfairness problem well, especially when the number of negative samples is large, which would hamper the effect of graph clustering.

3 Proposed Method

In this section, we detail how our proposed CueGCL achieves graph clustering. Specifically, we first construct a basic *Graph Contrastive Learning* framework in Section 3.1. Next, based on the node embeddings encoded by GCN in Graph Contrastive Learning framework, we design a *Personalized Self-Training* strategy in Section 3.2. Meanwhile, we introduce a *clustering layer* on the embeddings from GCN to achieve the clustering of the downstream task (Section 3.3), and *align* the clustering space of the downstream task with the clustering space of the PeST (Section 3.3). The general framework of our model is shown in Figure 2.

Firstly, we introduce some notations used in this paper.

Given a network $\mathcal{G} = (\mathcal{V}, \mathcal{E}, \mathcal{X})$, where $\mathcal{V} = \{v_1, v_2, \dots, v_n\}$ denotes the set of nodes in network, $\mathcal{E} = \{e_{ij}\} \subseteq \mathcal{V} \times \mathcal{V}$ denotes the set of edges between nodes, $\mathcal{X} = \{\mathbf{x}_1, \mathbf{x}_2, \dots, \mathbf{x}_n\}$ denotes the set of node attributes and $\mathbf{x}_i \in \mathbb{R}^d$ ($i = 1, 2, \dots, n$) is the feature of v_i , d is the dimension of the node attribute. We denote the adjacency matrix of the network as $A \in \mathbb{R}^{n \times n}$ and the feature matrix as $\mathbf{X} \in \mathbb{R}^{n \times d}$.

3.1 Graph Contrastive Learning

Graph contrastive learning obtains high-quality semantic representations by pulling positive sample pairs $(\mathbf{x}_i, \mathbf{x}_i^+)$ closer and negative sample pairs $(\mathbf{x}_i, \mathbf{x}_k^-)$ further away in the embedding space. Thus, CueGCL minimizes the following objective function for every node in the graph:

$$\mathcal{L}_{cl}(\mathbf{x}_i) = -\ln \frac{e^{g_\theta(\mathbf{x}_i)^T g_\theta(\mathbf{x}_i^+) / \tau}}{e^{g_\theta(\mathbf{x}_i)^T g_\theta(\mathbf{x}_i^+) / \tau} + \sum_{k \sim \tilde{\mathcal{N}}_i} e^{g_\theta(\mathbf{x}_i)^T g_\theta(\mathbf{x}_k^-) / \tau}}, \quad (1)$$

where $g_\theta(\cdot)$ is a GCN [Kipf and Welling, 2016a] with its parameter θ and τ is temperature parameter. We mask node feature \mathbf{x}_i randomly and obtain the positive sample \mathbf{x}_i^+ , which is a kind of graph augmentation strategy. Here, $\tilde{\mathcal{N}}_i = \{v_k\} (k \neq i)$ is the negative sample set of node v_i .

3.2 Personalized Self-Training

Self-training intends to extract semantic information from unlabeled data by adding high-confidence prediction nodes and their labels from each class to the training set. Inspired by it, we propose an incremental sampling and personalized self-training (PeST) strategy in unsupervised scenarios, as shown in Figure 3. Moreover, we demonstrate its effectiveness in experimental and theoretical aspects, respectively.

Implementation details. In contrast to general self-training algorithms that explore high-confidence node prediction results [Sun *et al.*, 2020], we choose to sample the medoids of each cluster in the embedding space for self-training and add them to the training set incrementally. Particularly, after each t epoch (i.e. the sampling frequency of medoids), one sampling is performed in the embedding space, and the obtained K medoid vectors are added to the training set, where K refers to the number of clusters in the graph and can be obtained by some non-parametric methods [Kulis and Jordan, 2012; Jiang *et al.*, 2011]. We use the K-medoids [Park and Jun, 2009] algorithm to obtain the real node v_j in each cluster center with the following objective function:

$$\sum_{i=1}^n \min_{j \in U_i} d(v_i, v_j) = \sum_{i=1}^n \min_{j \in U_i} \|g_\theta(\mathbf{x}_i) - g_\theta(\mathbf{x}_j)\|_2, \quad (2)$$

where $U_l = U_{l-1} \setminus M_{l-1}$ is the set of nodes that are not selected as the medoid in $(l * t)$ -th epoch and t represents the sampling frequency of medoids, l represents the sampling times. Also, we obtain $M_l = \{m_{l,0}, m_{l,1}, \dots, m_{l,K-1}\}$ as the selected K medoids in $(l * t)$ -th epoch. In graph clustering scenario, we do not have any label information in advance. Thus the subscript corresponding to the medoid vector

is directly assigned to its own label (i.e. $label(m_{l,i}) = i$), and the label set is denoted as $N_l = \{0, 1, \dots, K-1\}$. Therefore, in the T -th (i.e. $T = L * t$) epoch, we obtain the training set $M^T = \bigcup_{l=1}^L M_l$ and its label set $N^T = \bigcup_{l=1}^L N_l$. In order to learn the distribution of personalized features for each cluster, our CueGCL minimizes the following cross-entropy objective function \mathcal{L}_{st} :

$$\mathcal{L}_{st} = -\frac{1}{|M^T|} \sum_{i \in M^T} \sum_{n=0}^{K-1} y_{i,n} \ln \hat{y}_{i,n}. \quad (3)$$

Here, $y_{i,n} = 1$ if node i is the medoid of cluster n and 0 otherwise, indicating the n -th element of the one-hot label vector \mathbf{y}_i . $\hat{y}_{i,n}$ is the n -th element of the prediction label vector $\hat{\mathbf{y}}_i$ and it calculates as:

$$\hat{\mathbf{y}}_i = MLP(g_\theta(\mathbf{x}_i)), \quad (4)$$

where MLP is a two-layer fully connected neural network. Here, the role of the MLP is to generate the predicted label with semantic information. In addition, the incremental sampling strategy allows the more central medoids to be added in the training set earlier, thus our model could capture the personalized features of each cluster more accurately, as shown in Figure 3.

The reason why we choose to sample the medoids of each cluster for self-training is that this approach satisfies the following three essential principles:

1. The set of nodes is selected to be representative. General self-training algorithms tend to choose high-confidence nodes to join the training set, yet these nodes do not necessarily contain the critical information to train, especially the cluster-level semantic information. K-medoids can obtain better cluster centers, as theoretically demonstrated in [Wu *et al.*, 2019], thus allowing our model to capture cluster-level personalized information effectively.
2. The class information of the selected nodes is relatively precise. We select the medoids of each cluster since the confidence of their class is higher than other nodes. From Figure 3, we could show that our PeST module can be regarded as the contrastive learning of debiased negative samples, considering the selection of the medoids with less bias. It achieves a more accurate cluster-level discriminative role compared to the general contrastive learning algorithm. Thus our model only needs a small number of negative samples in GCL.
3. The set of nodes is selected to ensure class balance. The balanced sampling of medoids allows our model to learn more equally the information of each cluster in the graph, which guarantees the fairness of graph clustering to a degree.

More details about the PeST module, including its effectiveness and scalability as well as the reasons for using K-medoids, can be found in the **Appendix F**¹.

¹For detailed information on the appendix, please refer to the uploaded **supplementary materials**.

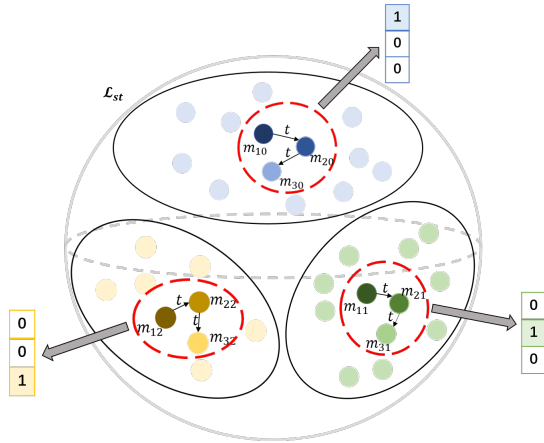


Figure 3: An illustration of incremental sampling and personalized self-training strategy. The deeper the color of the mediod, the more central it is.

Experimental and Theoretical Analysis. In the following, we will demonstrate experimentally and theoretically the effectiveness of our self-training strategy.

In Figure 4, we study the effectiveness of our PeST module by *modularity* metric, which measures the compactness of the cluster structure [Newman, 2006]. It can be observed that with the removal of the self-training module from our CueGCL, the modularity tends to decrease as training, which validates that our PeST module allows for a more compact structure within the clusters. More specifically, our model learns the personalized features of each cluster, so its embedding space has better cluster properties than those of the general contrastive learning method.

In theory, our PeST strategy is equivalent to adaptively drawing closer nodes of the same cluster, as formally proposed in Theorem 3.1.

Theorem 3.1. *An undirected graph \mathcal{G} has n nodes $\mathcal{V} = \{v_1, \dots, v_n\}$, and $\mathbf{H}_i^{(t)}$ ($\mathbf{H}_i^{(0)} = \mathbf{x}_i$) is the embedding of node v_i after t times message propagating and aggregation. And $\mathbf{y}_k \in \mathbb{R}^K$ is an one-hot label vector, where $y_k^{(k)} = 1$ is the k -th element of \mathbf{y}_k . Assume that node v_i belongs to cluster k , then we have $\forall \epsilon > 0, \exists T \in \mathbb{N}^+$, such that $\forall t > T$, then $\|\mathbf{H}_i^{(t)} - \mathbf{y}_k\|_2 \leq \epsilon$.*

Proof. Please refer to **Appendix B** for the complete proof. \square

The above theorem demonstrates that all nodes of the same cluster adaptively converge to a specified center. These center vectors are two-by-two orthogonal and span to a standard orthogonal space.

Summary: We use the K-medoids algorithm to incrementally extract the medoids of each cluster such that the clustering space converges to a set of standard orthogonal bases in the Euclidean space by optimizing the cross-entropy loss.

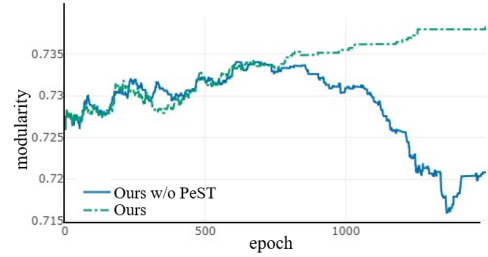


Figure 4: Effectiveness of our PeST module on Citeseer.

The PeST module allows us to obtain a node embedding space that is **tight within the cluster** and **sparse between the clusters**.

3.3 Aligned Graph Clustering

In this subsection, we propose an aligned graph clustering layer and jointly optimize it with graph contrastive learning and personalized self-training module. Based on the DEC algorithm [Xie *et al.*, 2016], we add the learnable cluster centers in downstream task to the self-training, in order to align them with the cluster medoids in PeST.

Clustering Layer. To obtain the graph clustering results, we develop a clustering layer. At first, we compute a soft assignment between the node embedding $g_\theta(\mathbf{x}_i)$ and the cluster center parameter μ_k . The similarity between them is measured by the Student's t -distribution Q as follows:

$$q_{ik} = \frac{\left(1 + \|g_\theta(\mathbf{x}_i) - \mu_k\|^2 / \alpha\right)^{-\frac{\alpha+1}{2}}}{\sum_j \left(1 + \|g_\theta(\mathbf{x}_i) - \mu_k\|^2 / \alpha\right)^{-\frac{\alpha+1}{2}}}, \quad (5)$$

where α is the degree of freedom of the t -distribution and q_{ik} can be interpreted as the probability of assigning node i to cluster k . We normally set $\alpha = 1$ and initialize the cluster centers $\{\mu_k\}_{k=1}^K$ by K-means. Secondly, we define the L_{clus} as the KL divergence loss between the soft assignments Q and the target distribution P as follows:

$$L_{clus} = KL(P||Q) = \sum_i \sum_k p_{ik} \log \frac{p_{ik}}{q_{ik}}, \quad (6)$$

where p_{ik} is the target distribution P with higher confidence assignments defined as follows:

$$p_{ik} = \frac{q_{ik}^2 / f_k}{\sum_k q_{ik}^2 / f_k}, \quad (7)$$

where $f_k = \sum_i q_{ik}$ is the soft cluster frequency.

Alignment Module. The clustering space of the downstream task is inconsistent with that in PeST, which will cause the information in PeST to be useless or even harmful to our downstream task. So we align these two spaces to reduce the interference of this inconsistent information on downstream tasks. Specifically, we add $C = \{\mu_k\}_{k=1}^K$ to the training set for self-training, similar to Section 3.2. Then, we minimize the following cross-entropy objective function \mathcal{L}_{al} :

$$\mathcal{L}_{al} = -\frac{1}{|C|} \sum_{i \in C} \sum_{n=0}^{K-1} y_{i,n} \ln \hat{y}_{i,n}. \quad (8)$$

Method	Input	Cora		Citeseer		PubMed		Cornell		Texas		Avg. Rank		
		ACC	NMI	ACC	NMI	ACC	NMI	ACC	NMI	ACC	NMI	ACC	NMI	
TA	SC	A	36.7	12.6	23.8	5.5	52.8	9.7	23.6	2.6	22.1	6.4	16.2	16.8
	K-means	X	49.2	32.1	54.0	30.5	59.5	31.5	21.3	3.6	23.4	10.4	14.4	11.6
GNN-A	MinCutPool (ICML'20)	(A, X)	49.0	41.0	53.7	29.5	52.1	21.4	42.1	11.9	50.5	11.8	10.8	10.2
	DMoNn (JMLR'23)	(A, X)	51.7	47.3	38.5	30.3	35.1	25.7	42.6	<u>12.5</u>	46.3	9.9	11.0	9.4
GA	VGAE (NIPS'16)	(A, X)	50.2	32.9	46.7	26.0	63.0	22.9	39.7	6.9	38.5	13.5	12.2	12.0
	ARGA (IJCAI'18)	(A, X)	64.0	44.9	57.3	35.0	66.8	30.5	36.4	7.1	42.5	15.5	11.2	9.0
	ARVGA (IJCAI'18)	(A, X)	64.0	45.0	54.4	26.1	69.0	29.0	38.6	8.3	41.3	<u>15.8</u>	9.6	8.8
	DAEGC (IJCAI'19)	(A, X)	69.4	50.6	64.5	36.4	68.7	28.3	35.0	7.4	52.3	12.4	7.4	8.8
	VGAER (AAAI'22)	(A, X)	45.3	29.7	30.2	21.7	30.1	22.3	29.5	6.2	26.2	3.0	15.8	15.6
	DDGAE (ESWA'24)	(A, X)	73.7	55.5	68.2	41.7	69.1	<u>33.1</u>	32.7	6.1	44.5	11.3	7.0	7.6
CA	CommDGI (CIKM'20)	(A, X)	66.1	52.8	62.1	39.8	63.2	30.6	39.3	7.2	53.0	11.4	7.8	8.2
	MVGRL (ICML'20)	(A, X)	73.6	58.8	68.1	43.2	<u>69.2</u>	32.0	38.3	8.9	41.5	9.5	7.2	<u>6.0</u>
	GDCL (IJCAI'21)	(A, X)	74.7	58.9	<u>69.7</u>	44.8	68.4	32.7	<u>45.3</u>	7.9	<u>55.7</u>	8.5	<u>3.4</u>	<u>6.0</u>
	gCool (WWW'22)	(A, X)	72.3	55.8	63.8	34.6	67.8	30.3	33.9	7.6	43.7	9.3	9.2	9.4
	S ³ -CL (AAAI'23)	(A, X)	73.9	58.0	68.8	43.7	69.0	32.3	42.7	9.4	50.3	8.1	4.4	6.2
	HSAN (AAAI'23)	(A, X)	<u>75.1</u>	<u>59.0</u>	69.2	<u>45.9</u>	68.6	31.5	41.2	8.1	52.8	7.6	4.4	6.4
CA	CueGCL (Ours)	(A, X)	77.9	60.5	71.4	47.2	71.2	36.8	46.1	13.6	56.7	17.1	1.0	1.0
	Gain		+2.8	+1.5	+1.7	+1.3	+2.0	+3.7	+0.8	+1.1	+1.0	+1.3	+2.4	+5.0

Table 2: The average performance of graph clustering with ACC and NMI on Cora, Citeseer, PubMed, Cornell, and Texas. The bold and underlined text indicates the optimal and suboptimal results, respectively. The Avg. Rank denotes the mean value across all five datasets for the rank among all methods about a specific metric.

Here, $y_{i,n} = 1$ if $i = n$ and 0 otherwise, indicating the n -th element of the one-hot label vector \mathbf{y}_i . $\hat{y}_{i,n}$ is the n -th element of the prediction label vector $\hat{\mathbf{y}}_i$ and it calculates as:

$$\hat{\mathbf{y}}_i = MLP(\boldsymbol{\mu}_i). \quad (9)$$

We align the clustering space in the downstream task with that in the representation space, which achieves more consistent node embeddings. Moreover, the cluster centers $\{\boldsymbol{\mu}_k\}_{k=1}^K$ are learnable, which means they can be optimized continuously during the training process. This provides additional training paradigms for our CueGCL to learn the personalized characteristics of each cluster, thereby enhancing the generalization capability of our model.

3.4 Joint Optimization

Consequently, we jointly graph contrastive learning, personalized self-training, and aligned graph clustering in an end-to-end trainable framework for more salient cluster structures. The overall objective function of the proposed CueGCL is induced as:

$$\min \mathcal{L} = \frac{1}{n} \sum_{i=1}^n \mathcal{L}_{cl}(\mathbf{x}_i) + \gamma_{st} \mathcal{L}_{st} + \gamma_{clus} \mathcal{L}_{clus} + \gamma_{al} \mathcal{L}_{al}, \quad (10)$$

where $\gamma_{st}, \gamma_{clus}, \gamma_{al} > 0$ are trade-off parameters to balance the magnitudes between different loss items.

On the one hand, the node representations obtained by contrastive learning have better discriminative properties and improve the accuracy of class information, thus facilitating the PeST module. On the other hand, PeST makes the contrastive learning of negative samples more accurate and efficient. With the mutual promotion of the various modules in our CueGCL, we can both obtain discriminative node representations and fair graph clustering. The whole algorithm is summarized in Algorithm 1 in Appendix C.

4 Experiment

4.1 Experimental Setup

Datasets. In this paper, we perform experiments on various real networks with different scales widely used in unsupervised graph representation learning [Zhao *et al.*, 2021; Yuan *et al.*, 2023]. The five benchmark datasets are: Cora [Sen *et al.*, 2008], Citeseer [Rossi and Ahmed, 2015], PubMed [Namata *et al.*, 2012], Cornell and Texas [Pei *et al.*, 2019]. Their detailed information is shown in Appendix D.1.

Baseline. In order to verify the superiority of our model, we compare it with the current state-of-the-art algorithms as follows: (1) **Unsupervised Algorithms**, including (1.1) Traditional algorithms (**TA**): Spectral clustering (SC) [Amini *et al.*, 2013], K-means [MacQueen, 1967]; (1.2) GNN-based algorithms (**GNN-A**): MinCutPool [Bianchi *et al.*, 2020], DMoN [Tsitsulin *et al.*, 2023]; (1.3) Generative-based algorithms (**GA**): VGAE [Kipf and Welling, 2016b], ARGAs [Pan *et al.*, 2018], ARVGA [Pan *et al.*, 2018], VGAER [Qiu *et al.*, 2022], DAEGC [Wang *et al.*, 2019], DDGAE [Wu *et al.*, 2024]; (1.4) Contrastive-based algorithms (**CA**): CommDGI [Zhang *et al.*, 2020], MVGRL [Hassani and Khasahmadi, 2020], GDCL [Zhao *et al.*, 2021], gCool [Li *et al.*, 2022], S³-CL [Ding *et al.*, 2023], HSAN [Liu *et al.*, 2023]. (2) **Semi-Supervised Algorithms**, including Self-training algorithms (**SA**): Co-training [Li *et al.*, 2018], Union [Li *et al.*, 2018], M3S [Sun *et al.*, 2020].

Evaluation Metrics. Two evaluation metrics are used to measure the performance of various algorithms, namely Accuracy (ACC) and Normalized Mutual Information (NMI). In addition, we adopt the F1 score (Micro-F1 and Macro-F1) to evaluate the fairness of clustering, which can comprehensively reflect the detection accuracy for each cluster.

Parameters Settings. Our experiments are run on the machine with two NVIDIA GeForce RTX 3090 Ti and the details of the hyperparameters are provided in Appendix D.2.

	N_{neg}	50		1500	
	Method	Micro-F1	Macro-F1	Micro-F1	Macro-F1
Cora	GDCL	36.4	34.4	11.9	9.4
	Ours	35.6	39.5	31.8	36.9
Citeseer	GDCL	32.3	31.3	4.6	3.9
	Ours	48.5	40.3	48.4	40.1
PubMed	GDCL	29.0	30.0	27.1	29.2
	Ours	39.2	30.9	40.4	32.0

Table 3: The F1 score of graph clustering on three graph datasets between previous contrastive-based SOTA GDCL and our CueGCL. We adopt the F1 score to evaluate the fairness in graph clustering, which can comprehensively reflect the detection accuracy for each cluster.

	Method	Label-free	Cora	Citeseer	PubMed
SA	Co-training	✗	73.5	62.5	72.7
	Union	✗	<u>75.9</u>	66.7	70.7
	M3S	✗	75.6	<u>70.3</u>	70.6
CA	Ours	✓	77.9	71.4	<u>71.2</u>

Table 4: The ACC of community detection on three graph datasets between self-training algorithms and our CueGCL.

4.2 Graph Clustering

We conduct the graph clustering experiment with our CueGCL and various comparison methods on five datasets 20 times and report the average results. We show the experimental results in Table 2, 3, and 4, where the **bold** and underlined text indicate the optimal and suboptimal results, respectively. It can be seen that our model outperforms all the comparison methods for different evaluation metrics and the specific analysis can be found in **Appendix D.3**. Additionally, for experiments on semi-supervised node classification, please refer to the **Appendix D.4**.

4.3 Ablation Study

To verify the effect of each module in our CueGCL, we conduct ablation experiments as shown in Table 5.

It is evident that our proposed personalized self-training and alignment module significantly improve the performance of our model for graph clustering. Examining row 1 and row 2 of this table, we can see an increase in performance of 5 to 6 points on the Cora when applying the PeST module. It indicates that this module does allow our model to learn the personalized features of each cluster. Moreover, the change in modularity shown in Figure 4 further validates the superiority of our PeST module, which leads to more compact cluster structures in embedding space.

4.4 Hyperparameter Analysis

To investigate the effect of each hyperparameter on our model, including the number of negative samples N_{neg} ; the sampling frequency t of Medoids and the dimension d of MLP ; the trade-off parameters γ_{st} and γ_{al} , we perform experiments and analysis on the Cora dataset. Due to page limitations, the details of the latter two experiments are provided in **Appendix E**.

Method	Cora		Citeseer		PubMed		Cornell		Texas	
	ACC	NMI	ACC	NMI	ACC	NMI	ACC	NMI	ACC	NMI
w/o \mathcal{L}_{st} & \mathcal{L}_{al}	69.9	55.1	69.9	44.4	69.0	35.2	43.7	9.5	44.3	12.4
w/o \mathcal{L}_{al}	75.1	59.9	70.8	46.0	70.2	35.2	45.0	11.9	52.9	14.5
w/o \mathcal{L}_{st}	75.0	59.5	70.6	46.2	70.1	34.5	44.6	12.3	50.4	13.7
CueGCL	77.9	60.5	71.4	47.2	71.2	36.8	46.1	13.6	56.7	17.1

Table 5: The effect of each module in our CueGCL for graph clustering on five graph datasets.

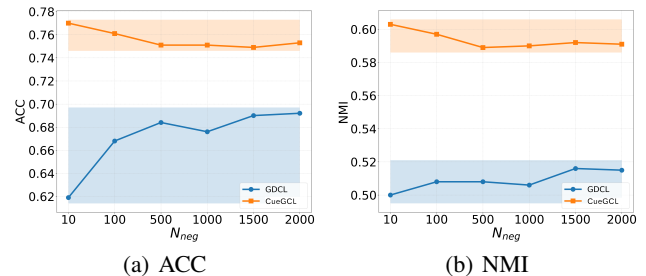


Figure 5: Graph clustering performance of different negative sample size N_{neg} on Cora. The shaded area indicates the fluctuation range of ACC and NMI.

The number of negative samples N_{neg} . Our CueGCL is a graph clustering method based on GCL, so we analyze the effect of N_{neg} and compare it with the GDCL. As can be seen from Figure 5, the performance of GDCL is sensitive to the change of N_{neg} . In general, when the number of negative samples is larger, the performance of GDCL is also better, which is in line with the general rule of the contrastive learning model. However, an excessive number of negative samples not only increases the training time, even worse but also leads to the class collision problem. On the contrary, our CueGCL is robust to N_{neg} on both ACC and NMI. In particular, our model achieves optimal results with $N_{neg} = 10$ on the Cora dataset. This is attributed to the PeST module, which is equivalent to the contrastive learning of debiased negative samples. Also, we calculate and compare the average accuracy of class information of medoids, with the highest at 86% for $N_{neg} = 10$.

5 Conclusion

In this paper, we propose a cluster-aware graph contrastive learning framework (CueGCL). The personalized self-training strategy can enhance the ability of our model to perceive clusters. In addition, we bring attention to the issue of unfairness in graph clustering when employing existing contrastive learning algorithms. We propose a straightforward yet effective solution to address this concern, marking a novel contribution to the field. By jointly training the three modules of graph contrastive learning, personalized self-training, and aligned graph clustering, we finally obtain an ideal embedding space that is compact within the same cluster and sparse between the distinct clusters. Extensive experiments also demonstrate the superiority of our CueGCL.

References

- [Amini *et al.*, 2013] Arash A Amini, Aiyu Chen, Peter J Bickel, and Elizaveta Levina. Pseudo-likelihood methods for community detection in large sparse networks. *The Annals of Statistics*, 41(4):2097–2122, 2013.
- [Bianchi *et al.*, 2020] Filippo Maria Bianchi, Daniele Grattarola, and Cesare Alippi. Spectral clustering with graph neural networks for graph pooling. In *International conference on machine learning*, pages 874–883. PMLR, 2020.
- [Chung, 1997] Fan RK Chung. *Spectral graph theory*, volume 92. American Mathematical Soc., 1997.
- [Deng *et al.*, 2024] Bowen Deng, Tong Wang, Lele Fu, Sheng Huang, Chuan Chen, and Tao Zhang. Thesaurus: Contrastive graph clustering by swapping fused gromov-wasserstein couplings. *arXiv preprint arXiv:2412.11550*, 2024.
- [Ding *et al.*, 2023] Kaize Ding, Yancheng Wang, Yingzhen Yang, and Huan Liu. Eliciting structural and semantic global knowledge in unsupervised graph contrastive learning. In *Proceedings of the AAAI Conference on Artificial Intelligence*, volume 37, pages 7378–7386, 2023.
- [Hassani and Khasahmadi, 2020] Kaveh Hassani and Amir Hosein Khasahmadi. Contrastive multi-view representation learning on graphs. In *International Conference on Machine Learning*, pages 4116–4126. PMLR, 2020.
- [Hinton *et al.*, 2015] Geoffrey Hinton, Oriol Vinyals, and Jeff Dean. Distilling the knowledge in a neural network. *arXiv preprint arXiv:1503.02531*, 2015.
- [Hjelm *et al.*, 2018] R Devon Hjelm, Alex Fedorov, Samuel Lavoie-Marchildon, Karan Grewal, Phil Bachman, Adam Trischler, and Yoshua Bengio. Learning deep representations by mutual information estimation and maximization. In *International Conference on Learning Representations*, 2018.
- [Hu *et al.*, 2020] Weihua Hu, Matthias Fey, Marinka Zitnik, Yuxiao Dong, Hongyu Ren, Bowen Liu, Michele Catasta, and Jure Leskovec. Open graph benchmark: Datasets for machine learning on graphs. *Advances in neural information processing systems*, 33:22118–22133, 2020.
- [Jiang *et al.*, 2011] Bin Jiang, Jian Pei, Yufei Tao, and Xuemin Lin. Clustering uncertain data based on probability distribution similarity. *IEEE Transactions on Knowledge and Data Engineering*, 25(4):751–763, 2011.
- [Kipf and Welling, 2016a] Thomas N Kipf and Max Welling. Semi-supervised classification with graph convolutional networks. In *International Conference on Learning Representations*, 2016.
- [Kipf and Welling, 2016b] Thomas N Kipf and Max Welling. Variational graph auto-encoders. *NIPS Workshop on Bayesian Deep Learning*, 2016.
- [Kulis and Jordan, 2012] Brian Kulis and Michael I Jordan. Revisiting k-means: new algorithms via bayesian nonparametrics. In *Proceedings of the 29th International Conference on International Conference on Machine Learning*, pages 1131–1138, 2012.
- [Li *et al.*, 2018] Qimai Li, Zhichao Han, and Xiao-Ming Wu. Deeper insights into graph convolutional networks for semi-supervised learning. In *Thirty-Second AAAI conference on artificial intelligence*, 2018.
- [Li *et al.*, 2022] Bolian Li, Baoyu Jing, and Hanghang Tong. Graph communal contrastive learning. In *Proceedings of the ACM Web Conference 2022*, pages 1203–1213, 2022.
- [Li *et al.*, 2024a] Yuecheng Li, Jialong Chen, Chuan Chen, Lei Yang, and Zibin Zheng. Contrastive deep nonnegative matrix factorization for community detection. In *ICASSP 2024-2024 IEEE International Conference on Acoustics, Speech and Signal Processing (ICASSP)*, pages 6725–6729. IEEE, 2024.
- [Li *et al.*, 2024b] Zhengdao Li, Yong Cao, Kefan Shuai, Yiming Miao, and Kai Hwang. Rethinking the effectiveness of graph classification datasets in benchmarks for assessing gnns. *arXiv preprint arXiv:2407.04999*, 2024.
- [Liu *et al.*, 2022] Hongrui Liu, Binbin Hu, Xiao Wang, Chuan Shi, Zhiqiang Zhang, and Jun Zhou. Confidence may cheat: Self-training on graph neural networks under distribution shift. In *Proceedings of the ACM Web Conference 2022*, pages 1248–1258, 2022.
- [Liu *et al.*, 2023] Yue Liu, Xihong Yang, Sihang Zhou, Xinwang Liu, Zhen Wang, Ke Liang, Wenxuan Tu, Liang Li, Jingcan Duan, and Cancan Chen. Hard sample aware network for contrastive deep graph clustering. In *Proceedings of the AAAI conference on artificial intelligence*, volume 37, pages 8914–8922, 2023.
- [MacQueen, 1967] J MacQueen. Classification and analysis of multivariate observations. In *5th Berkeley Symp. Math. Statist. Probability*, pages 281–297, 1967.
- [Namata *et al.*, 2012] Galileo Namata, Ben London, Lise Getoor, Bert Huang, and U Edu. Query-driven active surveying for collective classification. In *10th international workshop on mining and learning with graphs*, volume 8, page 1, 2012.
- [Newman, 2006] Mark EJ Newman. Modularity and community structure in networks. *Proceedings of the national academy of sciences*, 103(23):8577–8582, 2006.
- [Oord *et al.*, 2018] Aaron van den Oord, Yazhe Li, and Oriol Vinyals. Representation learning with contrastive predictive coding. *arXiv preprint arXiv:1807.03748*, 2018.
- [Pan *et al.*, 2018] Shirui Pan, Ruiqi Hu, Guodong Long, Jing Jiang, Lina Yao, and Chengqi Zhang. Adversarially regularized graph autoencoder for graph embedding. In *Proceedings of the 27th International Joint Conference on Artificial Intelligence*, pages 2609–2615, 2018.
- [Park and Jun, 2009] Hae-Sang Park and Chi-Hyuck Jun. A simple and fast algorithm for k-medoids clustering. *Expert systems with applications*, 36(2):3336–3341, 2009.
- [Pei *et al.*, 2019] Hongbin Pei, Bingzhe Wei, Kevin Chen-Chuan Chang, Yu Lei, and Bo Yang. Geom-gcn: Geomet-

- ric graph convolutional networks. In *International Conference on Learning Representations*, 2019.
- [Qiu *et al.*, 2022] Chenyang Qiu, Zhaoci Huang, Wenzhe Xu, and Huijia Li. Vgaer: graph neural network reconstruction based community detection. *arXiv preprint arXiv:2201.04066*, 2022.
- [Rossi and Ahmed, 2015] Ryan Rossi and Nesreen Ahmed. The network data repository with interactive graph analytics and visualization. In *Proceedings of the AAAI conference on artificial intelligence*, volume 29, 2015.
- [Saunshi *et al.*, 2019] Nikunj Saunshi, Orestis Plevrakis, Sanjeev Arora, Mikhail Khodak, and Hrishikesh Khandeparkar. A theoretical analysis of contrastive unsupervised representation learning. In *International Conference on Machine Learning*, pages 5628–5637. PMLR, 2019.
- [Sen *et al.*, 2008] Prithviraj Sen, Galileo Namata, Mustafa Bilgic, Lise Getoor, Brian Galligher, and Tina Eliassi-Rad. Collective classification in network data. *AI magazine*, 29(3):93–93, 2008.
- [Shiao *et al.*, 2023] William Shiao, Uday Singh Saini, Yozen Liu, Tong Zhao, Neil Shah, and Evangelos E. Papalexakis. CARL-G: clustering-accelerated representation learning on graphs. In *Proceedings of the 29th ACM SIGKDD Conference on Knowledge Discovery and Data Mining, KDD 2023, Long Beach, CA, USA, August 6-10, 2023*, pages 2036–2048. ACM, 2023.
- [Sun *et al.*, 2020] Ke Sun, Zhouchen Lin, and Zhanxing Zhu. Multi-stage self-supervised learning for graph convolutional networks on graphs with few labeled nodes. In *Proceedings of the AAAI Conference on Artificial Intelligence*, volume 34, pages 5892–5899, 2020.
- [Thakoor *et al.*, 2021] Shantanu Thakoor, Corentin Tallec, Mohammad Gheshlaghi Azar, Mehdi Azabou, Eva L Dyer, Remi Munos, Petar Veličković, and Michal Valko. Large-scale representation learning on graphs via bootstrapping. In *International Conference on Learning Representations*, 2021.
- [Tsitsulin *et al.*, 2023] Anton Tsitsulin, John Palowitch, Bryan Perozzi, and Emmanuel Müller. Graph clustering with graph neural networks. *Journal of Machine Learning Research*, 24(127):1–21, 2023.
- [Velickovic *et al.*, 2019] Petar Velickovic, William Fedus, William L Hamilton, Pietro Liò, Yoshua Bengio, and R Devon Hjelm. Deep graph infomax. *ICLR (Poster)*, 2(3):4, 2019.
- [Von Luxburg, 2007] Ulrike Von Luxburg. A tutorial on spectral clustering. *Statistics and computing*, 17(4):395–416, 2007.
- [Wang *et al.*, 2019] Chun Wang, Shirui Pan, Ruiqi Hu, Guodong Long, Jing Jiang, and Chengqi Zhang. Attributed graph clustering: a deep attentional embedding approach. In *Proceedings of the 28th International Joint Conference on Artificial Intelligence*, pages 3670–3676, 2019.
- [Wu *et al.*, 2019] Yuexin Wu, Yichong Xu, Aarti Singh, Yiming Yang, and Artur Dubrawski. Active learning for graph neural networks via node feature propagation. *arXiv preprint arXiv:1910.07567*, 2019.
- [Wu *et al.*, 2024] Xunlian Wu, Wanying Lu, Yining Quan, Qiguang Miao, and Peng Gang Sun. Deep dual graph attention auto-encoder for community detection. *Expert Systems with Applications*, 238:122182, 2024.
- [Xiao *et al.*, 2024] Teng Xiao, Huaisheng Zhu, Zhengyu Chen, and Suhang Wang. Simple and asymmetric graph contrastive learning without augmentations. *Advances in Neural Information Processing Systems*, 36, 2024.
- [Xie *et al.*, 2016] Junyuan Xie, Ross Girshick, and Ali Farhadi. Unsupervised deep embedding for clustering analysis. In *International conference on machine learning*, pages 478–487. PMLR, 2016.
- [Yuan *et al.*, 2023] Mengyi Yuan, Minjie Chen, and Xiang Li. Muse: Multi-view contrastive learning for heterophilic graphs. In *Proceedings of the 32nd ACM International Conference on Information and Knowledge Management*, pages 3094–3103, 2023.
- [Zhang *et al.*, 2020] Tianqi Zhang, Yun Xiong, Jiawei Zhang, Yao Zhang, Yizhu Jiao, and Yangyong Zhu. Comdgi: community detection oriented deep graph infomax. In *Proceedings of the 29th ACM International Conference on Information & Knowledge Management*, pages 1843–1852, 2020.
- [Zhang *et al.*, 2023] Zehua Zhang, Shilin Sun, Guixiang Ma, and Caiming Zhong. Line graph contrastive learning for link prediction. *Pattern Recognition*, 140:109537, 2023.
- [Zhao *et al.*, 2021] Han Zhao, Xu Yang, Zhenru Wang, Erkun Yang, and Cheng Deng. Graph debiased contrastive learning with joint representation clustering. In *IJCAI*, pages 3434–3440, 2021.
- [Zhu *et al.*, 2020] Yanqiao Zhu, Yichen Xu, Feng Yu, Qiang Liu, Shu Wu, and Liang Wang. Deep graph contrastive representation learning. *arXiv preprint arXiv:2006.04131*, 2020.
- [Zhu *et al.*, 2021] Yanqiao Zhu, Yichen Xu, Feng Yu, Qiang Liu, Shu Wu, and Liang Wang. Graph contrastive learning with adaptive augmentation. In *Proceedings of the Web Conference 2021*, pages 2069–2080, 2021.

To further elaborate on the ideas and results in our paper, this **supplementary material** provides additional details omitted from the main text.

A Additional Related Work

Graph Self-Training. Graph self-training is an important technique in semi-supervised learning that aims to fully exploit the value of data from unlabelled nodes in the graph. The authors in [Li *et al.*, 2018] propose self-training approaches including Co-training and Union to train graph convolutional network (GCN), which samples predicted labels of nodes with high confidence and adds them to the training set. M3S [Sun *et al.*, 2020] adopts a multi-stage self-training framework with a deep clustering algorithm. DR-GST [Liu *et al.*, 2022] considers recovering the distribution of the original labeled graph dataset when introducing the augmented data from self-training. Graph self-training methods can enhance the performance of the model for downstream tasks by improving the generalization of the GCN, but there are fewer self-training mechanisms for unsupervised graph representation learning. Furthermore, due to their limited representation modeling ability, they do not perform as well as our models, even though they use a small number of labels.

B Proof of Theorem 3.1

Theorem B.1 (Theorem 3.1 Restated). *An undirected graph \mathcal{G} has n nodes $\mathcal{V} = \{v_1, \dots, v_n\}$, and $\mathbf{H}_i^{(t)}$ ($\mathbf{H}_i^{(0)} = \mathbf{x}_i$) is the embedding of node v_i after t times message propagating and aggregation. And $\mathbf{y}_k \in \mathbb{R}^K$ is an one-hot label vector, where $y^{(k)} = 1$ is the k -th element of \mathbf{y}_k . Assume that node v_i belongs to cluster k , then we have $\forall \epsilon > 0, \exists T \in \mathbb{N}^+$, such that $\forall t > T$, then $\|\mathbf{H}_i^{(t)} - \mathbf{y}_k\|_2 \leq \epsilon$.*

Proof. Given the layer-wise propagation rule of GCN is

$$\mathbf{H}^{(t+1)} = \phi(\tilde{\mathbf{D}}^{-\frac{1}{2}} \tilde{\mathbf{A}} \tilde{\mathbf{D}}^{-\frac{1}{2}} \mathbf{H}^{(t)} \mathbf{W}),$$

where $\tilde{\mathbf{A}} = \mathbf{A} + \mathbf{I}$ is the adjacency matrix of \mathcal{G} with added self-loops in each node and \mathbf{I} is the identity diagonal matrix. $\tilde{\mathbf{D}}_{ii} = \sum_j \tilde{\mathbf{A}}_{ij}$ and \mathbf{W} is weight matrix of GCN. $\mathbf{H}^{(t)} \in \mathbb{R}^{n \times d_t}$ is the node embedding matrix in t -th layer, $\mathbf{H}^{(0)} = \mathbf{X} \in \mathbb{R}^{n \times d}$. ϕ is the activation function, such as Relu. Here for a easy proof, we assume that $\phi(x) = x$ and $\mathbf{W} = \mathbf{I}$. So, We can rewrite the GCN layer as

$$\mathbf{H}^{(t+1)} = \tilde{\mathbf{D}}^{-\frac{1}{2}} \tilde{\mathbf{A}} \tilde{\mathbf{D}}^{-\frac{1}{2}} \mathbf{H}^{(t)} = (\mathbf{I} - \mathbf{L}_{sym}) \mathbf{H}^{(t)},$$

where $\mathbf{L}_{sym} = \tilde{\mathbf{D}}^{-\frac{1}{2}} \tilde{\mathbf{L}} \tilde{\mathbf{D}}^{-\frac{1}{2}}$ is the symmetrically normalized Laplacian matrix and $\tilde{\mathbf{L}} = \tilde{\mathbf{D}} - \tilde{\mathbf{A}}$.

Given that each node in the graph \mathcal{G} has a self-loop, it can be concluded that there are no bipartite components in the graph. Consequently, it follows that the eigenvalues of \mathbf{L}_{sym} are all contained within the interval $[0, 2)$ [Chung, 1997]. As \mathbf{L}_{sym} is a real symmetric matrix, it is found to have n eigenvalues, which may include instances of repeated eigenvalues.

Additionally, we can derive a set of n orthogonal eigenvectors, denoted as $\{\mathbf{e}_j\}_{j=1}^n$.

Assume that \mathcal{G} has w connected components $\{C_i\}_{i=1}^w$ and define indication vector $\mathbf{1}_i$ as follows:

$$\mathbf{1}_i^{(j)} = \begin{cases} 1, & v_j \in C_i \\ 0, & v_j \notin C_i \end{cases}.$$

From [Von Luxburg, 2007], we know that the eigenspace of \mathbf{L}_{sym} corresponding to the eigenvalue of 0 is spanned by $\{\mathbf{D}^{-\frac{1}{2}} \mathbf{1}_i\}_{i=1}^w$. It is easy to know that if node v_i and v_j in the same connected component, we have

$$\forall k \in \{1, \dots, w\}, \quad \mathbf{1}_k^{(i)} - \mathbf{1}_k^{(j)} = 0.$$

Let $(\lambda_1, \dots, \lambda_n)$ denote the eigenvalue of matrix $\mathbf{I} - \mathbf{L}_{sym}$. Since the eigenvalues of \mathbf{L}_{sym} stand in $[0, 2)$, we have

$$-1 < \lambda_1 < \lambda_2 < \dots < \lambda_{n-w} < \lambda_{n-w+1} = \dots = \lambda_n = 1.$$

If node v_i and node v_j are in the same connected component, we can rewrite $\mathbf{H}_i^{(t)} - \mathbf{H}_j^{(t)}$ as

$$\begin{aligned} & \mathbf{H}_i^{(t)} - \mathbf{H}_j^{(t)} \\ &= \left[(\mathbf{I} - \mathbf{L}_{sym})^t \mathbf{H}^{(0)} \right]_i - \left[(\mathbf{I} - \mathbf{L}_{sym})^t \mathbf{H}^{(0)} \right]_j \\ &= \left[(\mathbf{I} - \mathbf{L}_{sym})^t (\mathbf{e}_1, \dots, \mathbf{e}_n) \hat{\mathbf{H}} \right]_i - \left[(\mathbf{I} - \mathbf{L}_{sym})^t (\mathbf{e}_1, \dots, \mathbf{e}_n) \hat{\mathbf{H}} \right]_j \\ &= \left[\lambda_1^t (\mathbf{e}_1^{(i)} - \mathbf{e}_1^{(j)}), \dots, \lambda_{n-w+1}^t \times 0, \dots, \lambda_n^t \times 0 \right] \hat{\mathbf{H}}, \end{aligned}$$

where $\{\mathbf{e}_j\}_{j=1}^n$ are the eigenvectors of \mathbf{L}_{sym} (also $\mathbf{I} - \mathbf{L}_{sym}$) and $\mathbf{e}_j^{(i)}$ is the i -th element of \mathbf{e}_j . $\hat{\mathbf{H}}$ is the coordinate matrix of $\mathbf{H}^{(0)}$ in the n -dimensional orthogonal space spanned by eigenvectors of \mathbf{L}_{sym} .

We set $\mathbf{H}_j^{(t)} = \mathbf{M}_k^{(t)}$ and $\mathbf{M}_k^{(t)}$ is the embedding of the medoid of the cluster k . Thus,

$$\left\| \mathbf{H}_i^{(t)} - \mathbf{M}_k^{(t)} \right\|_2 = \sqrt{\sum_{j=1}^n \left[\sum_{m=1}^{n-w} \lambda_m^t (\mathbf{e}_m^{(i)} - \mathbf{e}_m^{(k)}) \hat{\mathbf{H}}_{mj} \right]^2}.$$

Since $-1 < \lambda_1 < \lambda_2 < \dots < \lambda_{n-w} < 1$, we have

$$\forall \epsilon > 0, \exists T_1 \in \mathbb{N}^+, \text{ s.t. } \forall t > T_1, \text{ then } \left\| \mathbf{H}_i^{(t)} - \mathbf{M}_k^{(t)} \right\|_2 \leq \frac{\epsilon}{2}.$$

According to the equivalence of cross entropy and L2 norm in the gradient optimization [Hinton *et al.*, 2015], when we minimize the cross entropy loss \mathcal{L}_{st} in Eq. (3) from the main text, it is actually equivalent to optimizing the following L2 norm,

$$\min \left\| \mathbf{M}_k^{(t)} - \mathbf{y}_k \right\|_2.$$

So, we have

$$\forall \epsilon > 0, \exists T_2 \in \mathbb{N}^+, \text{ s.t. } \forall t > T_2, \text{ then } \left\| \mathbf{M}_k^{(t)} - \mathbf{y}_k \right\|_2 \leq \frac{\epsilon}{2}.$$

In summary, according to the triangle inequality of norm, we have

$$\forall \epsilon > 0, \exists T = \max(T_1, T_2), \text{ s.t. } \forall t > T, \text{ then } \left\| \mathbf{H}_i^{(t)} - \mathbf{y}_k \right\|_2 \leq \left\| \mathbf{H}_i^{(t)} - \mathbf{M}_k^{(t)} \right\|_2 + \left\| \mathbf{M}_k^{(t)} - \mathbf{y}_k \right\|_2 \leq \epsilon.$$

□

C Algorithm 1

Algorithm 1 CueGCL

Input: Graph \mathcal{G} , Iterations *epoch*, Sampling Frequency *t*

Output: Node Embeddings and Clustering Results

- 1: Initialize model parameters.
 - 2: **for** $T = 1$ **to** *epoch* **do**
 - 3: Encode node embeddings by GCN $g_\theta(\cdot)$.
 - 4: **if** $T \% t == 0$ **then**
 - 5: Sample and update the medoid set M^T by Eq. (2).
 - 6: Update distribution Q and P by Eq. (5), (7) respectively.
 - 7: **end if**
 - 8: Update model parameters by minimizing Eq. (10) through SGD.
 - 9: **end for**
-

D More Details About the Experiment

D.1 The Detail of Datasets

We conduct experiments on five commonly used datasets for graph learning, using the default dataset splits in PyG². These datasets primarily include two types of networks and specific details are outlined below.

- **Cora** [Sen *et al.*, 2008]: A citation network with 2708 nodes and 5429 edges. Each node represents a paper in the field of machine learning, and each edge represents a citation relationship between two papers. The feature of a node is represented as a 1433-dimension binary vector, which indicates the presence of the corresponding word. Each node in this graph is classified into one of the following seven classes: Case Based, Genetic Algorithms, Neural Networks, Probabilistic Methods, Reinforcement Learning, Rule Learning, and Theory.
- **Citeseer** [Rossi and Ahmed, 2015]: A citation network with 3312 nodes and 4732 edges. Each node represents a paper in the field of computer science, and each edge represents a citation relationship between two papers. The feature of a node is represented as a 3703-dimension binary vector. Each node in this graph is classified into one of the following six classes: Agents, AI, DB, IR, ML, and HCI.

²<https://pytorch-geometric.readthedocs.io/>

- **PubMed** [Namata *et al.*, 2012]: A citation network with 19717 nodes and 44338 edges. Each node represents a paper in the field of diabetes, and each edge represents a citation relationship between two papers. The feature of a node is represented as a 500-dimension Term Frequency Inverse Document Frequency (TFIDF) vector. Each node in this graph is classified into one of the following three classes: Diabetes Mellitus, Experimental, Diabetes Mellitus Type 1, and Diabetes Mellitus Type 2.
- **Cornell and Texas** [Pei *et al.*, 2019]: Two webpage networks with 183 nodes. Each node represents a web page collected from computer science departments of various universities, and each edge represents a hyperlink between two web pages. The feature of a node is represented as a 1703-dimension bag-of-words representation. Each node in both graphs is classified into one of the following five classes: student, project, course, staff, and faculty.

D.2 Hyperparameter Setting

Following the suggestions in DEC [Xie *et al.*, 2016], we pre-train the encoder of our framework. The important hyperparameters for the graph clustering task are shown in Table 6.

D.3 Experimental Analysis of Graph Clustering

1. The results in Table 2 show that deep learning methods based on GCN for graph clustering are significantly better than traditional clustering algorithms (i.e. K-means, SC). Since GCN makes more reasonable use of graph topology and node properties. Additionally, we observed that the contrastive-based approach (i.e. MVGRL, GDCL, S^3 -CL, and HSAN) generally outperforms the generative-based approach (i.e. VGAE, ARG, ARVGA, DAEGC, VGAER, and DDGAE). This can be attributed to the fact that the generative-based approach tends to learn feature-level information, whereas the contrastive-based approach learns more node-level information, making it better suitable for downstream graph clustering tasks.
2. Our proposed CueGCL outperforms all comparison methods including contrastive-based algorithms on all five datasets. For example, on the Cora, our model significantly outperforms the previous SOTA GDCL by 3.2% and 1.6% in ACC, and NMI, respectively. It is possible that GDCL could not consider the cluster structure, while our CueGCL explicitly extracts cluster-level information through the integration of PeST and AGC. Furthermore, compared to S^3 -CL, which utilizes prototype contrastive learning by directly minimizing the distance between prototypes and nodes, our PeST provides a more natural and unbiased approach to cluster structure learning. Based on the experiment results from Figure 4 and Table 2, it can be concluded that our CueGCL can better solve the **Challenge I** raised in the introduction.
3. To verify the fairness of contrastive learning methods in graph clustering, we compare our CueGCL with the previous contrastive-based SOTA GDCL in Table 3. As the

Dataset	Backbone	Hyperparameter
Cora	GCN	epochs: 1000, lr: $5e-5$, $hidden_{GCN}$: 512, layers: 1, τ : 0.5, N_{neg} : 10, t: 50, d: 256, γ_{st} : 0.01, γ_{al} : 0.001
Citeseer	GCN	epochs: 1000, lr: $5e-5$, $hidden_{GCN}$: 512, layers: 1, τ : 0.5, N_{neg} : 50, t: 150, d: 256, γ_{st} : 0.0005, γ_{al} : 0.0001
PubMed	GCN	epochs: 300, lr: $5e-5$, $hidden_{GCN}$: 220, layers: 1, τ : 0.2, N_{neg} : 10, t: 30, d: 256, γ_{st} : 10, γ_{al} : 0.001
Cornell	GCN	epochs: 300, lr: $1.5e-6$, $hidden_{GCN}$: 200, layers: 1, τ : 0.5, N_{neg} : 4, t: 10, d: 128, γ_{st} : 10, γ_{al} : 0.01
Texas	GCN	epochs: 50, lr: $8e-6$, $hidden_{GCN}$: 512, layers: 1, τ : 0.5, N_{neg} : 5, t: 10, d: 512, γ_{st} : 0.1, γ_{al} : 0.1

Table 6: The hyperparameters for our model on five graph datasets.

negative sample size increases and class collision worsens, the fairness of graph clustering based on GDCL receives different degrees of impact on the three datasets. By the way, since the PubMed dataset has only three classes (clusters), GDCL is slightly affected compared to the other two datasets. In contrast, our model reaches significantly higher F1 scores than the GDCL, especially when the negative sample size is large. This indicates our model equally achieves considerable precision when detecting each cluster and solves the problem in **Challenge II** that arises when applying the contrastive framework to graph clustering.

4. Co-training, Union, and M3S are semi-supervised learning algorithms for self-training. During their training process, we use label rates of 2%, 3%, and 0.1% w.r.t. Cora, Citeseer, and PubMed. It is worth mentioning that the common label rates for these three datasets in node classification tasks are 5.2%, 3.6%, and 0.3%. As shown in Table 4, our model is almost superior to three other methods in terms of ACC when applied to community detection, even though we do not use any label information. This is because our contrastive-based CueGCL fully utilizes the information of abundant unlabeled nodes. Besides, the nodes we sample in the PeST module are more representative of each cluster than those in other self-training methods.

D.4 Node Classification

To further validate the quality of the embedding space, we conducted node classification experiments based on the standard linear evaluation protocol [Velickovic *et al.*, 2019; Hu *et al.*, 2020]. The average accuracy and standard deviations over 10 runs are reported in Table 7. Specifically, we compared CueGCL with the two categories of state-of-the-art algorithms: (1) Supervised: MLP, GCN [Kipf and Welling, 2016a]. (2) Unsupervised + Fine-Tuning: VGAE [Kipf and Welling, 2016b], DGI [Velickovic *et al.*, 2019], MVGRL [Hassani and Khasahmadi, 2020], GCA [Zhu *et al.*, 2021], BGRL [Thakoor *et al.*, 2021], S^3 -CL [Ding *et al.*, 2023] and GraphACL [Xiao *et al.*, 2024].

We observed that our CueGCL outperforms other methods in terms of average classification performance across the three datasets. This indicates that cluster-level information can also enhance the performance of supervised downstream tasks.

Method	Cora	Citeseer	PubMed	Avg. Rank
MLP	56.11±0.34	56.91±0.42	71.35±0.05	10.0
GCN	81.50±1.30	70.30±0.28	78.80±2.90	7.67
VGAE	76.30±0.21	66.80±0.23	75.80±0.40	9.0
DGI	82.30±0.60	71.80±0.70	76.80±0.60	7.0
MVGRL	83.03±0.27	72.75±0.46	79.63±0.38	4.33
GCA	82.93±0.42	72.19±0.30	80.79±0.45	4.67
BGRL	82.70±0.60	71.10±0.60	79.60±0.50	6.33
S^3 -CL	<u>84.50±0.40</u>	<u>74.60±0.40</u>	80.80±0.30	<u>2.33</u>
GraphACL	84.20±0.31	73.63±0.22	82.02±0.15	<u>2.33</u>
CueGCL	86.42±0.21	74.88±0.62	<u>81.93±0.14</u>	1.33

Table 7: The performance of node classification with ACC on Cora, Citeseer, and PubMed. The bold and underlined text indicates the optimal and suboptimal results, respectively. The Avg. Rank denotes the mean value across three datasets for the rank among all methods.

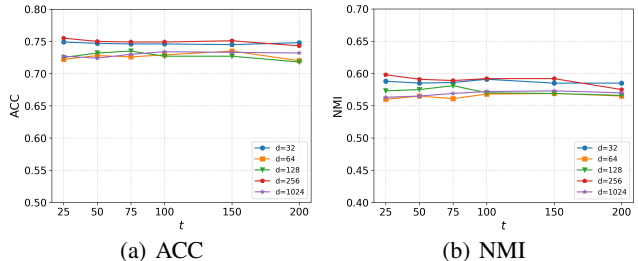


Figure 6: Clustering performance of different t and d on Cora.

E Additional Hyperparameter Analysis

E.1 The sampling frequency t of Medoids and the dimension d of MLP

In the PeST module, we sample the medoid vectors of each cluster in every t epochs and generate their prediction labels by using the MLP. The dimension of the hidden layer in MLP is noted by d . Then, we conduct graph clustering at t and d from [25, 50, 75, 100, 150, 200] and [32, 64, 128, 256, 1024] respectively, and report the results in Figure 6. As can be seen, the performance of our model remains mostly stable. Furthermore, we can observe that the performance of our CueGCL is slightly higher when $t = 25$ compared to the other t . This is due to the fact that more medoid vectors are added to the training set thus allowing our model to learn more information about each cluster in the graph.

Method	Cora		Citeseer		PubMed		Cornell		Texas	
	ACC	NMI	ACC	NMI	ACC	NMI	ACC	NMI	ACC	NMI
Ours with K-means	74.1	59.1	70.3	45.8	69.6	34.4	42.6	11.3	48.7	12.4
Ours with K-medoids	77.9	60.5	71.4	47.2	71.2	36.8	46.1	13.6	56.7	17.1

Table 8: The effect of clustering algorithms in PeST on five graph datasets.

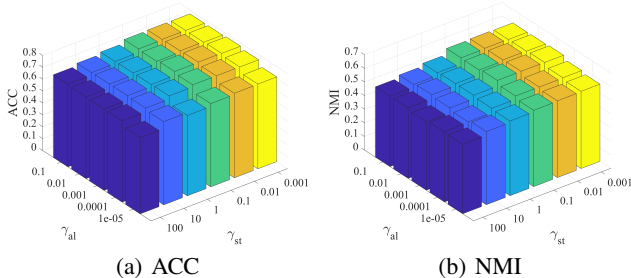


Figure 7: Clustering performance of different trade-off parameters γ_{st} and γ_{al} on Cora.

E.2 The trade-off parameters γ_{st} and γ_{al}

First, we perform experiments and analyses on the trade-off parameters γ_{st} and γ_{al} , as shown in Figure 7. We can observe that our CueGCL achieves optimal performance on Cora by adopting γ_{st} and γ_{al} to be 0.01 and 0.001, respectively. For different γ_{st} , our model is essentially stable on both ACC and NMI. In addition, as γ_{al} gradually increases from 10^{-5} , the performance of our model shows an increasing trend. This also demonstrates the importance of the alignment module in AGC, which indeed improves the generalization ability of our model. Overall, our CueGCL achieves commendable performance with a reasonable combination of trade-off parameters and is robust for both γ_{st} and γ_{al} .

F More Details About the PeST

F.1 On the effectiveness and scalability

Our proposed PeST is actually more unbiased and efficient contrastive learning of negative samples (as shown in Figure 3). The unbiasedness stems from the reliability of the class information. For example, the accuracy of the medoids’ class information used for self-training on PubMed remained at **100%** throughout the entire training process. In addition, it is evident the time complexity of negative sample learning in general GCL algorithms is $O(n^2)$. While our model’s time complexity in negative sample learning is $O(n \times N_{neg}) + O(n \times K) \approx O(n)$, where N_{neg} represents the number of negatives sampled from $\tilde{\mathcal{N}}_i$, and K represents the number of clusters in the network. Benefiting from the PeST module, only a few negative samples are necessary in our contrastive learning framework. So both N_{neg} and K are much smaller than the number of nodes in the network (i.e. n), particularly for large-scale graphs.

F.2 Why do we use K-medoids in the PeST module instead of other clustering algorithms such as K-means?

In our study, we choose the K-medoids algorithm for extracting cluster information and for self-training, based on the following considerations:

- **Motivation Explanation:** As you can see, in lines 268-291 of the paper, we detailed the three main motivations for choosing K-medoids.
- **Theoretical Guarantee:** A significant feature of K-medoids is its use of real nodes from the graph as centroids, providing a theoretical guarantee that the cluster is high-quality from our method. According to lines 745-746 in Appendix B, we need to set $H_j^{(t)} = M_k^{(t)}$, which requires $M_k^{(t)}$ to be the real centroid node (since H represents nodes in the graph), while the centroids obtained by K-means are the mean of nodes within a cluster and may not correspond to any real node.
- **Optimization Loss:** Related work [Wu *et al.*, 2019] has demonstrated that K-medoids can result in a lower optimization loss compared to other similar clustering methods, such as K-Center, which is effective for various loss functions including cross-entropy we use in Eq. (3).

As shown in Table 8, we replace K-medoids with K-means in our framework, the comparative results show that the performance is better when using K-medoids.